PAPER • OPEN ACCESS

A portable kit for refractive-index studies: refraction and critical angle in solids and liquids

To cite this article: Muhammad Nazreen Samuri *et al* 2026 *Phys. Educ.* **61** 015039

OPEN ACCESS
PAPER
Phys. Educ. **61** (2026) 015039 (14pp)
iopscience.org/ped

A portable kit for refractive-index studies: refraction and critical angle in solids and liquids

Muhammad Nazreen Samuri[1], **Yap Wing Fen**[1,2,*], **Nurul Huda Osman**[1], **Muhammad Fauzi Md Hairi**[1] **and Muhammad Fahmi Anuar**[2]

[1] Department of Physics, Faculty of Science, Universiti Putra Malaysia, 43400 UPM Serdang, Selangor, Malaysia
[2] Functional Nanotechnology Devices Laboratory, Institute of Nanoscience and Nanotechnology, Universiti Putra Malaysia, 43400 UPM Serdang, Selangor, Malaysia

E-mail: yapwingfen@upm.edu.my

Abstract
This paper presents a portable and simple refractive index kit that lets students study refraction, refractive index, and the critical angle in both solids and liquids. In schools, refraction is typically taught using a ray box that produce bright and dim rays, making refraction hard to observe. In addition, the activity also requires drawing lines on paper to trace the rays, which is time consuming and slows the process of teaching and learning. To overcome this problem, the portable refractive index kit uses a monochromatic 532 nm laser beam with a rotating mount and a fixed protractor as the sample stage, making the rays easy to observe without paper tracing and speeding up the lesson. In addition, the kit also offers added value by including a liquid container that enables refractive-index studies of liquids using the same geometry as solids without changing the setup. These additions save time, improve repeatability, and enable clear measurements for both solids and liquids within a single lesson. Refractive index is estimated using Snell's law from a straight-line Snell plot, and the critical angle for total internal

* Author to whom any correspondence should be addressed.

reflection is used as a built-in check. Results for typical classroom samples are $n = 1.56$ for glass, $n = 1.33$ for water, and $n = 1.45$ for cooking oil, with critical angles of 40.17°, 48.75°, and 43.60° respectively. The uncertainties of n, obtained from standard error analysis, range between ± 0.01 and ± 0.02 depending on the measurement method. This project contributed to physics education by providing a low cost, accurate and easy to obtain experimental kit for schools. This innovation adds value to teaching and learning by improving visibility, reducing setup time, and enabling fair comparison between solids and liquids within a single lesson.

Keywords: refractive index, Snell's law, critical angle, total internal reflection, portable refractive index kit

1. Introduction

Refraction is the change in direction of light at a boundary between two media of different refractive indices [1]. The refractive index of each material quantifies how much the speed of light is reduced with respect to the reference speed within vacuum. The greater the refractive index, the slower the light travels within that medium [2]. In Malaysia, this topic is introduced in Form 4 Physics within Chapter 6 Light and Optics, which presents two classroom investigations of light bending, namely Experiment 6.1 (Angle of refraction depends on angle of incidence) and Activity 6.3 (Critical angle and total internal reflection (TIR)) [3]. This is a sound approach because laboratory activities provide a clear entry point to optics and are more effective when common mistakes are anticipated and corrected early [4]. However, students often face practical challenges when running conventional refraction and TIR experiments in schools [5].

To carry out bending of light experiments in schools, teachers commonly use a ray box or a bulb as the light source. However, the beams from a typical ray box or bulb are often dim and broad in a bright classroom, which makes them a poor choice as the main light source for accurate refraction learning [6]. As a result, students struggle to see and measure the ray paths under normal classroom lighting, which reduces the effectiveness of teaching and learning [7]. To address this problem, the traditional ray box can be replaced with monochromatic light [8, 9]. Monochromatic light provides a bright, narrow single-wavelength beam that reduces colour dispersion, improves visibility, and yields more precise angle readings for refraction and TIR [8, 9]. Hence, in this study, monochromatic light is introduced to improve visibility and produce clearer, and more reliable angle measurements. The equipment presented allows the study of ordinary refraction and TIR within a single lesson.

Another problem when conducting refraction experiments in schools is slow and time-consuming, making it difficult to complete a single experiment within one lesson [10]. This happens because students need to draw the incident ray, the normal line and angle markings on the paper before they can measure the angles of incidence and refraction [11]. To address this problem, teachers can get everything ready before class and follow a clear step-by-step procedure, which shortens setup, speeds the activity, and leaves more time to explain the ideas behind the measurements [12]. This approach improves the quality of teaching and learning by freeing lesson time through clear and efficient setups as it gives teachers more space to explain key ideas and check students' understanding [13]. Hence, this study introduces a simple classroom approach that shortens setup and supports accurate angle measurement within a single lesson.

Other than that, another problem in school refraction work is that experiments to find refractive index are often done only with a glass block [14]. In the Form 4 textbook, students use a rectangular glass block in Experiment 6.1 to explore refraction from air to glass, and a semicircular glass block in Activity 6.3 to determine the critical angle and observe TIR. As a result, students learn only the refractive index of glass and miss the chance to compare other media such as water and may not notice that both refractive index and critical angle vary with the medium [15, 16]. As an alternative, an innovation that enables students to measure the refractive index of liquids and compare the results with solids can be introduced. With this step, students can test liquids alongside solids, see that refractive index and critical angle vary with the medium, and connect the lab to everyday cases more easily [17]. Hence, this study presents an innovation that enables measurement of the refractive index of liquids and solids in one lesson and supports clear, repeatable angle readings.

To address classroom constraints, this project introduces focused improvements that make refraction work easy to observe, quicker to carry out, and easier to link to key ideas [18, 19]. First, this project used a monochromatic portable laser to produce a narrow, high-contrast beam that improves visibility and supports more precise angle readings for refraction and TIR in normal classroom light. For example, Kutzner reported that a low-cost laser level produces a thin, bright ray that improves contrast on paper and makes angle readings more consistent in classroom optics [9]. Next, this project included simple measurement guides and a short step-by-step sheet to shorten setup and support quick, accurate angle readings. For example, a recent study designed a portable, low-cost experimental tool with clear procedures and teacher-validated usability that improved observation clarity and made classroom use more practical, which supports the value of streamlined instructions [20]. Lastly, this project introduced a liquid-testing component so students can measure the refractive index of liquids and compare the results with those of glass within one lesson [15, 17]. For example, Ladino and Rondón reported a simple laser and tank method that gives classroom-ready liquid refractive index values, which supports including a low-cost liquid module in this project [15]. Together, these additions create a compact refractive index kit that fits a single lesson, improves visibility, shortens setup, and enables side-by-side comparisons of solids and liquids, leading to clearer measurements and stronger understanding. Aside from these improvements, the equipment proposed in this project is economical and can be sourced from local bookstores and e-commerce websites. This makes it possible for schools in poor or remote areas to procure an experimental set and can eventually improve the quality of secondary school physics education. All components are low-cost and locally available (e.g. stationery or e-commerce suppliers), making the kit practical for resource-constrained schools and routine classroom use.

2. Theory

2.1. *Ray model and refractive index*

The ray model provides a simple framework for this topic because it treats light as straight lines. Refraction occurs when a ray crosses a flat boundary between two uniform media with refractive indices n_i and n_r. For consistency, all angles are measured from the normal at the point of incidence, as shown in figure 1, which labels the incident and refracted rays. The refractive index then describes how much light slows in a material relative to vacuum and is defined by:

$$n = \frac{c}{v}. \tag{1}$$

For a single-colour classroom laser, n can be treated as constant at this level of precision. A simple object-in-water analysis gives the same ray-model predictions and helps explain what we see when light goes from water to air [21].

2.2. *Snell's law and linearisation for measurement*

The relationship between the incident and refracted angles is given by Snell's law,

$$n_i \sin\theta_i = n_r \sin\theta_r. \tag{2}$$

Plotting sin θ_i (vertical axis) against sin θ_r (horizontal axis) yields a line with slope as shown in equation (3):

$$m = \frac{n_r}{n_i}. \tag{3}$$

With air outside the sample ($n_i \approx 1.000$), the slope directly estimates the sample index,

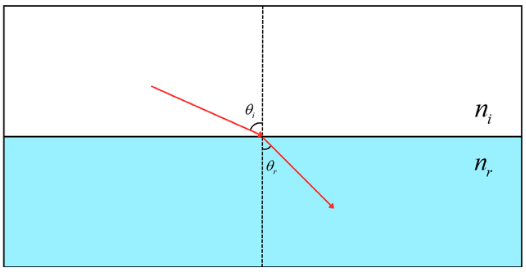

Figure 1. Ray model and angle conventions at a plane interface. The incident ray in medium n_i meets the boundary at angle θ_i; the refracted ray in medium n_r emerges at θ_r. Angles are measured from the normal.

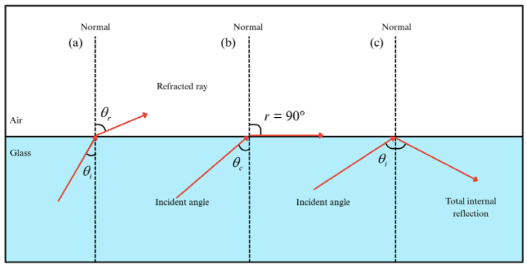

Figure 2. Critical angle and TIR at a medium–air boundary. (a) $\theta_i < \theta_c$: refraction; (b) $\theta_i = \theta_c$: refracted ray emerges at 90° (grazing) and (c) $\theta_i > \theta_c$: total internal reflection.

$m \approx n_{\text{sample}}$. If the plotting choice is reversed (sin θ_r vs sin θ_i), the slope becomes as shown in equation (4):

$$m \approx \frac{1}{n_{\text{sample}}}. \tag{4}$$

At a flat water–air interface, refraction makes submerged objects appear shallower, as shown in standard school ray diagrams and classroom studies [21]. For analysis, Snell's law is written in linear form by plotting sin θ_i (vertical axis) against sin θ_r (horizontal axis) and fitting two straight lines. The line constrained through the origin represents the ideal mo its slope gives the refractive index n. A second line with both slope and intercept also yields n and helps detect small alignment or zero-reading offsets. A small but non-zero intercept usually indicates a systematic bias rather than new physics, a point worth discussing with students [22]. Because the steps are straightforward, this linear treatment is common in school laboratories and in recent studies on quantitative measurement. In applied work, the same Snell-law framework supports camera calibration through flat water-air windows and improves underwater measurements and 3D reconstruction [23].

2.3. Critical angle and TIR

When light goes from a higher-index medium n_i, into a lower-index medium n_r, there is a limiting incidence angle called the critical angle, θ_c. At this angle the refracted ray does not enter the second medium; instead, it emerges at 90° to the normal and just grazes the boundary from Snell's law

$$\sin\theta_c = \frac{n_r}{n_i} \quad (n_i > n_r) \tag{5}$$

so, for a medium air boundary ($n_r \approx 1$), the refractive index is:

$$n \approx \frac{1}{\sin\theta_c}. \tag{6}$$

This single-parameter measurement complements the Snell-plot method and is especially helpful when angle readings near 90° on the refracted side are difficult. TIR occurs only when light goes from a higher to a lower refractive index and the internal incidence angle exceeds the critical angle, $\theta_i > \theta_c$. In classroom use, a semicircular glass block is arranged so the beam enters the curved face normally, which removes refraction on entry. The only angle to set is θ_i at the flat face, and the change across the three cases $\theta_i < \theta_c$, $\theta_i = \theta_c$ and $\theta_i > \theta_c$, as shown in figure 2. The critical angle, θ_c was identified at the just-grazing condition, after which the refractive index is found using the critical-angle relation from Snell's law. The portable single-geometry kit keeps the same alignment for solids and liquids, so θ_c can be measured and compared across media within one lesson.

2.4. Implications for a single-geometry classroom kit

Equations (3)–(6) provide two independent, curriculum-level ways to estimate n using one stable setup. The first method takes the slope from a Snell plot of sin θ_i versus sin θ_r. The second method finds the critical angle and uses equation (6) to calculate n. Using the same base alignment for both solids and liquids keeps the geometry constant and allows a direct comparison within the stated uncertainty. This practice is consistent with recent lab-learning studies and classroom reports on TIR-based refractive-index measurements and compact teaching kits. As a simple check, report two fits on the Snell plot: one line constrained through the origin and one with a free intercept. Any difference between the two helps reveal small alignment errors or wall-thickness effects before interpreting the results.

3. Methodology

3.1. Apparatus design and classroom constraints

This project consists of six main elements chosen to keep the geometry simple and the angle readings repeatable as shown in figure 3. At the centre is a fixed 360° protractor. It is used to define the origin of the normal, so every incident and refracted angle is read from the same point. Next, a standard rectangular glass block is used to study refraction in a solid and a clear acrylic cuboid container to study the refraction in liquids. Moreover, the laser beam is always aligned to the normal to the entry wall, so it travels straight to the exit face. Other than that, a low-power green laser pointer (532 nm) can be rotated in a smooth rotating mount. As the mount turns, the beam stays at constant height and remains centred on the protractor, which speeds up angle setting and removes the need to draw lines on paper. For the critical angle experiment, a semicircular glass container is included; the curved face ensures normal entry so only the flat face sets the internal incidence angle. In use, each sample is centred on the protractor origin and only the laser mount rotates, keeping the angle conventions visible and the alignment stable. All components are low-cost and portable, so the setup is practical for routine lessons and quick demonstrations.

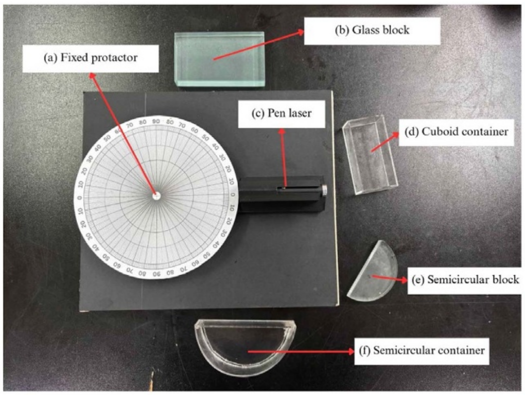

Figure 3. Complete refractive-index kit (a) fixed 1° protractor, (b) glass block, (c) rotating green laser (532 nm), (d) acrylic cuboid container, and (e)–(f) semicircular elements for critical angle.

3.2. Safety and materials

3.2.1. Light source. A low-power 532 nm green laser (Class 1 or 2 is recommended due to safety; Class 3 R requires additional institutional controls as it can unnecessarily impose hazards to the classroom environment) served as the source and was aligned tangentially to the semicircular elements to minimise refraction at the exit face [24]. It is noted that some students tend to be curious and can inadvertently harm themselves while carrying out the experiment. Therefore, lasers with too high powers or classified as restricted must not be used.

3.2.2. Refracting elements and beam. A standard glass block was placed at the centre of a fixed 1° resolution protractor. For liquids, a container was put in the same position so that the geometry did not change. The laser beam was set perpendicular to the entry wall so that it travelled straight inside the cell to the exit face. Before taking any liquid measurements, an empty container reading was taken to find the small angle shift caused by the wall thickness, noted as $\Delta\theta$. This $\Delta\theta$ was then subtracted from all liquid readings. Using the same layout for both solids and liquids keeps the normal and angle references the same, and the arrangement works for both refraction and TIR.

For the water and oil trials, this offset was subtracted from each θ_r before calculating sin θ_r for the Snell plot. The θ_r values in table 1 already include this baseline correction.

Table 1. Measured refraction data and derived quantities for glass, water, and cooking oil. Each θ_r value is the mean of three repeats. SD(θ_r) is the sample standard deviation across the three repeats at that angle. sin θ_i fixed by the experimental setting; sin θ_r computed from the mean θ_r. Uncertainties in n are handled in the text via propagation; we do not list a per-row n here to avoid double-counting when combining across angles.

Incident angle, θ_i (°)	Refracted angle, θ_r (°)								Refractive index, n			
	1st	2nd	3rd	Mean	SD θ_r (°)	SD θ_r (rad)	Sin θ_i	Sin θ_r	Tabular	SD (rad)	SE	Graphical
(a) Glass												
20	13	12	13	12.67	0.4714	0.0082	0.342	0.2193	1.56	0.0571	0.015	1.56
30	19	17	20	18.67	1.2472	0.0218	0.5	0.3201	1.56	0.1007		
40	25	24	25	24.67	0.4714	0.0082	0.6428	0.4173	1.54	0.0276		
50	29	28	30	29	0.8165	0.0143	0.766	0.4848	1.58	0.0406		
60	34	33	35	34	0.8165	0.0143	0.866	0.5592	1.55	0.0327		
(b) Water												
20	15	14	16	15	0.8165	0.0143	0.342	0.2588	1.32	0.0703	0.0091	1.33
30	22	22	23	22.33	0.4714	0.0082	0.5	0.38	1.32	0.0264		
40	29	28	28	28.33	0.4714	0.0082	0.6428	0.4746	1.35	0.0207		
50	35	35	35	35	0	0	0.766	0.5736	1.34	0		
60	41	40	40	40.33	0.4714	0.0082	0.866	0.6472	1.34	0.013		
(c) Oil												
20	14	13	13	13.33	0.4714	0.0082	0.342	0.2306	1.48	0.0515	0.0079	1.45
30	20	21	20	20.33	0.4714	0.0082	0.5	0.3475	1.44	0.0335		
40	26	26	27	26.33	0.4714	0.0082	0.6428	0.4436	1.45	0.0262		
50	32	33	32	32.33	0.4714	0.0082	0.766	0.5348	1.43	0.0211		
60	37	37	36	36.67	0.4714	0.0082	0.866	0.5972	1.45	0.018		

3.2.3. Workspace and handling. As with other experiments, the kit must be placed on a stable, level and clean workbench. Even small items, when falling or not well-handled, can cause injuries. The workbench should also be marked as appropriate. This is to prevent obstruction of the equipment by other items (e.g. notebooks, pencils). The kit, once not in use, must be disassembled and stored. The batteries must be removed and kept separately in accordance with local codes [25].

3.2.4. Rationale for green source. Green offers high-contrast in normal room light, aiding alignment and trace visibility. Small deviations from handbook refractive-index values are expected due to wavelength/temperature differences [26].

3.3. Experiment 1: Snell-plot method (glass, water, oil)

The sample was centred on a fixed 1° protractor in the portable kit, and the green laser on the rotating arm set nominal incidence angles of $\theta_i = 20°$, 30°, 40°, 50°, and 60°. For each setting, the refracted angle θ_r was read three times for the glass block.

The same steps were then repeated with the liquid container in the same holder. First with water, then with cooking oil. The liquid level was kept slightly above the beam so there was no refraction at the liquid–air surface. The beam was aligned normal to the entry wall so the path inside to the exit face was straight.

An empty-cell baseline was recorded to find the small wall-thickness shift $\Delta\theta$, and this $\Delta\theta$ was subtracted from all liquid θ_r readings before analysis. Data were processed using one convention. Compute sin θ_i and sin θ_r. Make a Snell plot with sin θ_i on the vertical axis and sin θ_r on the horizontal axis. Two straight-line fits were used. The line constrained through the origin gives the refractive index from the slope, reported as slope ± standard error (SE). The line with a free intercept serves as a check for small alignment or zero-reading offsets. For each angle, the three repeats were averaged, and the standard error of the mean was used for the error bars. This sequence keeps one geometry and one angle convention for solids and liquids, allowing side-by-side classroom comparison with the same portable kit, as shown in figure 4.

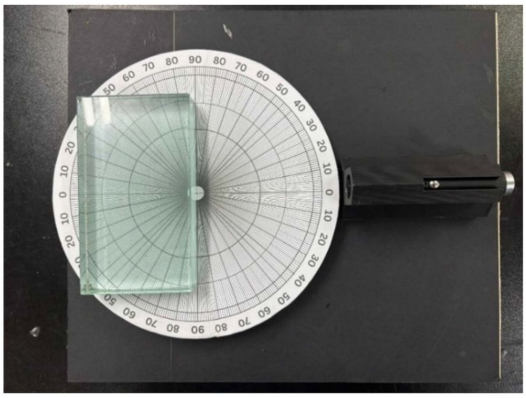

Figure 4. Snell-plot workflow: (i) angle readings at the protractor centre; (ii) empty-cell $\Delta\theta$ baseline; (iii) sin θ_i vs sin θ_r with origin-constrained fit for n (optional unconstrained check).

3.4. Experiment 2: Critical-angle and TIR methods (glass and liquids)

For solids, the semicircular glass block was aligned so the laser enters the curved face at normal incidence and reaches the flat face with no refraction on entry. The angle of incidence was increased until the angle of refraction became 90°. In other words, the refracted ray ran along the air-glass boundary. The angle of incidence was then recorded as the critical angle θ_c, as shown in figure 5. To make the grazing point clear, the classroom light was dimmed. The white card was placed on the flat face of the block to make the exiting ray easier to see. The knob was adjusted slowly in small steps near the critical point.

For liquids, the same geometry was used with the semicircular container filled first with water and then with cooking oil. This arrangement meets the higher-to-lower index condition for TIR, so the three cases are easy to spot: below θ_c a refracted spot appears in air, at θ_c the refracted ray skims along the surface, and above θ_c the refracted ray disappears and only the reflected ray remains inside the medium.

The critical angle was recorded three times for each medium. The mean value and its

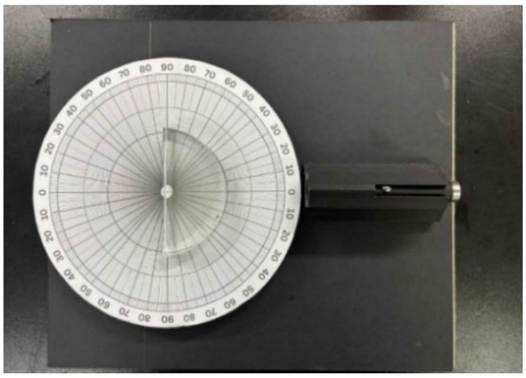

Figure 5. Experiment 2: geometry for determining θ_c and demonstrating TIR in solids (semicircular block) and liquids (semicircular container).

spread were used to report θ_c and its uncertainty. Refractive index was then calculated from equation (6). As a practical check, faces and windows were cleaned before each run, the normal line was marked clearly, and the protractor was read at eye level to avoid parallax.

These measurements provide an independent check on the Snell-plot results using the same setup. Small differences usually come from a zero offset on the scale, a slight wall tilt, a uniform wall thickness in the liquid cell, or a curved meniscus. With this simple procedure, solids and liquids can be compared in one lesson using one alignment.

3.5. Analysis summary, agreement, and reporting

In Experiment 1, separate straight lines were fitted for glass, water, and oil. For the origin-constrained model, the result is reported as $n = \text{slope} \pm$ Standard error. For the unconstrained model, both the fitted slope and the intercept are reported. Using one geometry and one angle convention lets students compare the index from the Snell plot with the index from the critical-angle method from Experiment 2, then judge whether the two values agree within the error bars. Small differences prompt useful checks: an intercept close to zero supports good alignment; a small non-zero intercept points to a constant offset such as a zero reading, a slight wall tilt, or a uniform wall-thickness effect. Averaging three reads per setting and reporting the standard error makes the uncertainty visible and keeps the comparisons of air across materials.

This style of analysis aligns with current laboratory guidance that asks students to compare data with models and act on those comparisons while treating uncertainty as part of the reasoning process [27]. Next, other research shows that repeated practice in making and acting on quantitative comparisons strengthens students' critical thinking and decision-making in laboratories [28, 29]. Finally, the approach mirrors recent classroom work on refractive-index measurements using TIR and compact apparatus suitable for school settings [30].

4. Results and discussion

4.1. Verification of Snell's law

For each medium, the refraction angle θ_r was measured three times at incidence angles $\theta_i = 20°$, $30°$, $40°$, $50°$, $60°$. The average value and standard error of the refraction angle were then calculated. If the light travels from air to the object, then $n_1 = 1$, $\theta_1 = \theta_i$, $\theta_2 = \theta_r$ and equation (2) becomes

$$n = \frac{\sin\theta_i}{\sin\theta_r}. \tag{7}$$

Since θ_i is fixed, we assume that $\Delta\theta_i$ is negligibly small and standard deviation (SD) of θ_r (in radians) is reflected as the uncertainty of n, according to [31],

$$\delta n = \left|\frac{\delta n}{\delta\theta_r}\right|\delta\theta_r = \frac{\sin\theta_i\cos\theta_r}{\sin^2\theta_r}\delta\theta_r. \tag{8}$$

Once the variation of n was computed for each θ_i, the overall variation of n can be found from

$$\delta n = \sqrt{\frac{N_1\delta n_1^2 + N_2\delta n_2^2 + \ldots + N_5\delta n_5^2}{N_1 + N_2 + \ldots + N_5}}. \tag{9}$$

Equation (9) expresses the variation of n as the SD, which can then be converted to the standard error of the mean (SE) using

$$SE(n) = \frac{\delta n}{\sqrt{N}} \tag{10}$$

where,

$$N = N_1 + N_2 + \ldots N_5. \tag{11}$$

Table 4.1 summarises the experimental data for each medium, including the mean refracted angles, their SDs, and the calculated refractive indices with their respective uncertainties. The refractive index for each incident angle was obtained using equation (7), and the uncertainty of n was determined from the propagation of error described in equation (8). The overall variation of n was then computed using equation (9), and the SE was derived from equation (10).

For glass, the mean refractive index obtained was

$$n_{\text{glass}} = 1.56 \pm 0.0150$$

for water,

$$n_{\text{water}} = 1.33 \pm 0.0091$$

and for oil,

$$n_{\text{oil}} = 1.45 \pm 0.0079.$$

These values are in good agreement with the standard refractive indices of glass ($n \approx 1.50$–1.55), water ($n \approx 1.333$), and vegetable oil ($n \approx 1.46$). The small deviations between the experimental and tabulated values can be attributed to measurement errors in the refraction angle, parallax error during angle reading, and surface irregularities of the samples.

As expected from Snell's Law, the refractive index remained nearly constant for different incident angles, indicating that the relationship between $\sin\theta_i$ and $\sin\theta_r$ is linear. This was further verified graphically by plotting $\sin\theta_i$ against $\sin\theta_r$, which produced a straight line passing through the origin. The slope of the best-fit line corresponds to the refractive index of the medium.

The close agreement between the tabular method and the graphical method demonstrates the reliability of the experimental setup and supports the validity of Snell's Law. Furthermore, the use of SE rather than only SD provides a more realistic measure of confidence in the mean refractive index value obtained from multiple observations.

To aid replication and classroom adoption, we also show the experimental layouts for the three media, as shown in figure 7.

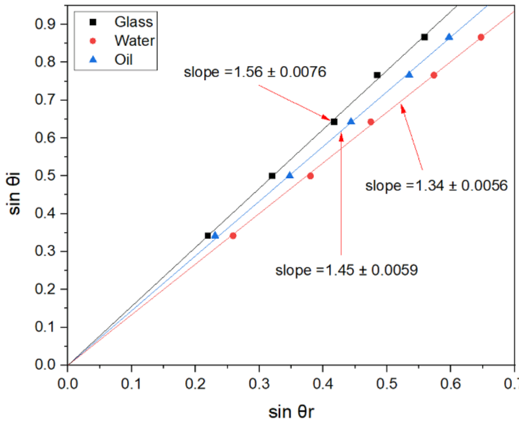

Figure 6. Linearised Snell's law: $\sin\theta_i$ vs $\sin\theta_r$ for glass, water and cooking oil. Lines are origin-constrained least-squares fits; slope $= n$. Reported values (slope $\pm$ SE): glass 1.56 ± 0.0076, water 1.34 ± 0.0056, oil 1.45 ± 0.0059.

4.2. Critical angle and TIR

Using the semicircular block and container geometry, the incident angle was increased until the refracted ray grazed the boundary, identifying the critical angle θ_c; the refractive index was then computed from equation (6). The measured critical angles were $\theta_c = 40.17°$ (glass), $48.75°$ (water), and $43.60°$ (oil). Uncertainties could be found using

$$\delta n = \left|\frac{\mathrm{d}n}{\mathrm{d}\theta_c}\right|\delta\theta_c = \frac{\cos\theta_c}{\sin^2\theta_c}\delta\theta_c. \tag{12}$$

Using equations (6) and (12) and assuming that the uncertainties of the protractor is 0.008728 rad, refractive indices were $n_{\text{Glass}} = 1.550 \pm 0.016$, $n_{\text{Water}} = 1.330 \pm 0.010$ and $n_{\text{Oil}} = 1.450 \pm 0.013$ (value $\pm$ SE). A protractor with smaller resolution will result in smaller uncertainties. Note again that students at school level are not encouraged to analyse the uncertainties until they sufficiently understand calculus. To reduce reading bias, θ_c was approached from both below and above. The two readings were averaged. This TIR approach is therefore easy and well-established.

This TIR approach is well established for classroom solids and liquids and provides an independent check against the Snell-plot values as shown in figure 8 and summarised in table 2.

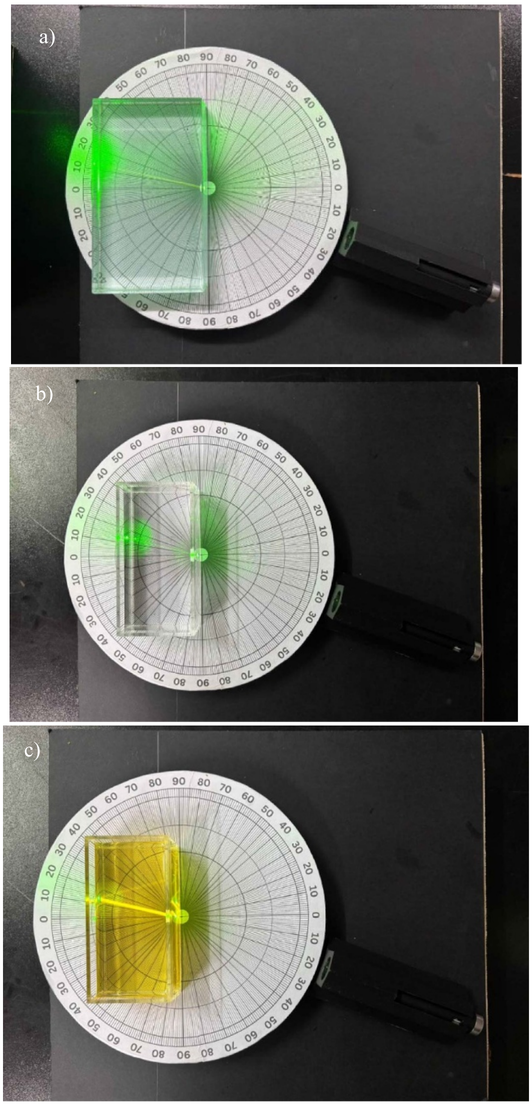

Figure 7. Experimental setups for measuring refraction in different media: (a) glass blocks, (b) cuboid container filled with water, and (c) cuboid container filled with cooking oil.

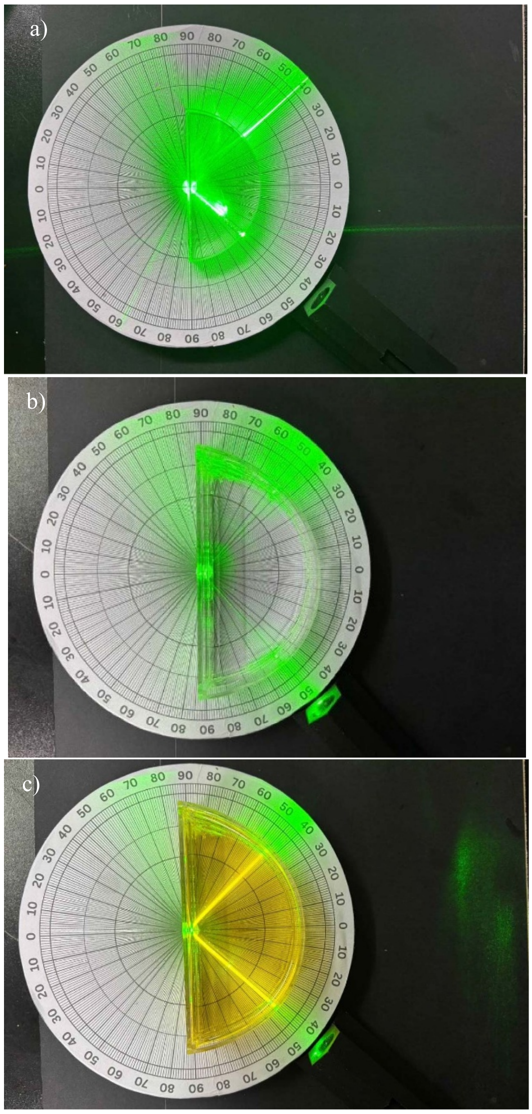

Figure 8. TIR for (a) glass; (b) water; and (c) cooking oil, showing the point at which the refracted ray emerges along the boundary and total internal reflection begins.

Common classroom errors such as parallax at the scale and small backlash in the rotating arm were limited by steady approach and multiple readings.

4.3. Agreement, uncertainty, and classroom relevance

Across glass, water, and oil, the portable kit gave consistent refractive-index values: the slope from the Snell plot and the value from the critical angle agreed within their stated uncertainties. For the Snell plot, results are reported as n = slope ± SE for the origin-constrained fit and as slope with intercept for the unconstrained fit, which also diagnoses small alignment bias. Using the two readings as a cross-check helps students draw conclusions from noisy data when uncertainty is taught and practiced deliberately [32]. This emphasis on uncertainty and comparison supports a shift from

Table 2. Critical angle (θ_c) and refractive index for glass, water and cooking oil.

Medium	Critical angle, θ_c (°)	Refractive index, n
Glass	40.17	1.550 ± 0.016
Water	48.75	1.330 ± 0.010
Cooking oil	43.60	1.450 ± 0.013

point-paradigm to set-paradigm reasoning about measurement in the physics laboratory [33].

4.4. Educational significance

The paired evidence invites students to compare measurements with their uncertainties, state agreement or discrepancy, and link visible ray paths to a quantitative model, as shown in figures 6 and 8 [34]. Quick extensions use the same single-geometry setup. One option is to record the ray paths with a smartphone and overlay a protractor to automate angle extraction [35]. Another is a short dispersion check by adding a second laser to compare refractive indices at two wavelengths [36]. With structured comparison prompts and short predict–measure–compare cycles, the activity aligns with evidence that such designs build critical-thinking skills in introductory laboratory. In addition, the proposed kit is also economical and can be built using items from local shops or ecommerce website. This will greatly benefit schools in deprived areas and will also improve the quality of science education. The kit is also suitable for use in engineering and science departments at universities. Instead of relying on expensive and fragile equipment, students can be encouraged to build a kit from scratch to improve their designing and laboratory skills.

4.5. Limitations and practical notes

Principal limitations at classroom precision include $1°$ scale resolution, small alignment errors, and residual wall-thickness effects in the container. These factors can bias θ_r and θ_c, so reporting slope $\pm$ SE (forced origin) and slope with intercept keep comparisons transparent. The shared-geometry design reduces confounds between methods, and the green (532 nm) beam remains clearly visible under ambient lighting, supporting safe, flexible classroom implementation, as shown in figure 6 and table 2 [37].

5. Conclusion

This project offers a practical way to address common problems in school refraction experiments, and it does so with simple, repeatable steps. Conventional setups often change alignment between solids and liquids, which leads to unclear angle conventions and lost lesson time. Therefore, the portable single-geometry kit keeps one stable alignment for both solids and liquids, and it uses the same angle convention throughout while removing refraction on entry. Consequently, two curriculum-level estimates of the refractive index can be obtained in the same apparatus, namely through a Snell plot and through the critical angle. In addition, a simple baseline step corrects small wall-thickness shifts, and an unconstrained line fit on the Snell plot helps diagnose zero-reading or alignment errors before results are interpreted. Because these design choices make the phenomena visible, students can see the three TIR cases clearly, compare the two independent estimates of n and judge agreement within uncertainty. Moreover, the procedures fit within a single lesson and use inexpensive parts, so they align with current recommendations for reasoning with data and uncertainty. Overall, the kit serves as a ready initiative for schools to improve optics teaching, reduce setup burden, and support more reliable, quantitative learning about refraction and the critical angle. Because all parts are inexpensive and widely available, the kit can be adopted quickly in typical school laboratories and teacher training workshops. A short Bill of Materials is provided in Appendix to guide teachers and laboratory technicians in assembling the kit, along with approximate component costs to emphasise its affordability and classroom reproducibility.

All raw angle tables and analysis spreadsheets are provided as supplementary files; figures can be regenerated from these files.

Data availability statement

All data that support the findings of this study are included within the article (and any supplementary files).

Acknowledgment

The authors gratefully acknowledge the financial support for this study from Universiti Putra Malaysia through Graduate Research Fellowship (GRF). The laboratory facilities provided by Applied Optics Laboratory (AOLAB), Faculty of Science, Universiti Putra Malaysia, were also acknowledged.

Funding statement

This research received no specific grant from any funding agency in the public, commercial, or not-for-profit sectors.

Conflict of interest

The authors declare that they have no known competing financial interests or personal relationships that could have appeared to influence the work reported in this paper.

Ethics statement

This study did not involve human participants, identifiable personal data, or animals; it reports bench-top measurements using standard instructional apparatus. Institutional ethics approval and participant consent were therefore not required.

Appendix. Cost of Equipment

No.	Item	Typical specification	Cost (RM)
1.	Fixed protractor	1° divisions (resolution 1°), PLA 3D Printing	40
2.	Pen laser	⩽1 mW, 532 nm, **Class 1–2**	12
3.	Rotating mount	PLA 3D Printing	25
4.	Glass block	11 × 6 × 2 cm	20
5.	Semicircular block	Radius ≈ 4 cm	12
6.	Cuboid container	9 × 4.5 × 3 cm	10
7.	Semicircular Container	Radius ≈ 6 cm	25
8.	Plywood	Kit body structure	16
Total			**160**

ORCID iDs

Muhammad Nazreen Samuri 0009-0005-8621-4927
Yap Wing Fen 0000-0003-3475-7469

Received 9 September 2025, in final form 1 December 2025
Accepted for publication 17 December 2025
https://doi.org/10.1088/1361-6552/ae2e73

References

[1] Jääskeläinen M, Lombard M and Zülicke U 2011 Refraction in spacetime *Am. J. Phys.* **79** 672–7
[2] Arbab A I 2016 Propagation of photons in a medium and refractive index *Optik* **127** 10758–65
[3] Kementerian Pendidikan Malaysia 2019 Buku Teks Fizik Tingkatan 4 *KSSM Bab 6 "Cahaya dan Optik"*
[4] Masters M and Grove T 2010 Active learning in intermediate optics through concept building laboratories *Am. J. Phys.* **78** 485
[5] Kaltakci-Gurel D, Eryilmaz A and McDermott L C 2016 Identifying pre-service physics teachers' misconceptions and conceptual difficulties about geometrical optics *Eur. J. Phys.* **37** 045705
[6] Ashmann S, Anderson C W and Boeckman H 2016 Helping secondary school students develop a conceptual understanding of refraction *Phys. Educ.* **51** 045009
[7] Foley T, Pegram M, Jenkins Z, Hester B C and Burris J L 2015 Laser soap fountain *Phys. Teach.* **53** 10–12
[8] Chen Y, Kim H R, Ahn Y J and Kim J B 2022 Geometric optical experiments using water mixed with highlighter ink *Phys. Teach.* **60** 765–7
[9] Kutzner M 2013 The laser level as an optics laboratory tool *Phys. Teach.* **51** 532–4
[10] Sokolowski A 2013 Conceptualization of light refraction *Phys. Teach.* **51** 110–1
[11] Rodrigues M and Simeão Carvalho P 2014 Teaching optical phenomena with Tracker *Phys. Educ.* **49** 671–7
[12] Yu Y, Zhang Y and Duan W 2015 Benefits and disadvantages of assay kits in experimental education *Proc. Int. Conf. on Management Science, Education Technology, Arts, Social Science and Economics (MSETASSE 2015)* pp 777–80
[13] Ramadan W A and El-Tawargy A S 2024 An economic, compact apparatus to verify the laws of reflection and refraction *Phys. Teach.* **62** 520–3
[14] Lanchester P C 2014 Studies of the reflection, refraction and internal reflection of light *Phys. Educ.* **49** 532–6
[15] Ladino L A and Rondón S H 2015 Refractive index of a transparent liquid *Phys. Educ.* **50** 295–8
[16] Ceuppens S, Deprez J, Dehaene W and De Cock M 2018 Tackling misconceptions in geometrical optics *Phys. Educ.* **53** 045020
[17] Santosa I E 2021 Measuring refractive index of a liquid with a spherical shape flask and Tracker *Phys. Educ.* **56** 065014
[18] Carli M 2023 Enhancing the use of the laboratory through action research in physics teacher communities *Phys. Rev. Phys. Educ. Res.* **19** 020162
[19] DeStefano P R and Widenhorn R 2024 Open-inquiry opens doors to intriguing optics experiments at home and in the classroom *Phys. Rev. Phys. Educ. Res.* **20** 010108
[20] Hairi M F M, Fen Y W, Yusof K A, Ismail M F I, Samuri M N, Kamarudin N and Khusaini K 2025 Revolutionizing experimental tools: innovative design to enhance classroom

usability *J. Pendidikan Fisika Indonesia* **21** 1–18
[21] Aprilia C and Irawan D 2024 Analyzing the refraction of light on an object in water *J. Front. Res. Sci. Eng.* **2** 30
[22] Grusche S and Wagner S 2016 Two different looks at Kepler's refraction experiment *Phys. Educ.* **51** 064001
[23] Pedersen M, Bengtson S H, Gade R, Madsen N and Moeslund T B 2018 Camera calibration for underwater 3D reconstruction based on ray tracing using Snell's law *2018 IEEE/CVF Conf. on Computer Vision and Pattern Recognition Workshops (CVPRW)* p 1491
[24] Galang J, Restelli A, Hagley E W and Clark C W 2010 A green laser pointer hazard NIST *Technical Note* 1668 p 9
[25] MacIsaac D 2017 Green laser safety *Phys. Teach.* **55** 446
[26] Sharpe L T, Stockman A, Jagla W and Jägle H 2005 A luminous efficiency function, $V^*(\lambda)$, for daylight adaptation *J. Vis.* **5** 948
[27] Kozminski J, Lewandowski H, Beverly N, Lindaas S, Deardorff D, Reagan A, Dietz R, Eblen-Zayas M, Williams J and Zwickl B 2014 *AAPT Recommendations for the Undergraduate Physics Laboratory Curriculum* (American Association of Physics Teachers)
[28] Holmes N G, Wieman C E and Bonn D A 2015 Teaching critical thinking *Proc. Natl Acad. Sci. USA* **112** 11199–204
[29] Holmes N G, Olsen J, Thomas J L and Wieman C E 2020 Developing scientific decision making by structuring and supporting student agency *Phys. Rev. Phys. Educ. Res.* **16** 010109
[30] Van Keuren E R 2005 Refractive index measurement using total internal reflection *Am. J. Phys.* **73** 611–5
[31] Taylor J R 1997 *Introduction to Error Analysis: The Study of Uncertainties in Physical Measurements* 2nd edn (University Science)
[32] Wan T 2023 Investigating student reasoning about measurement uncertainty and ability to draw conclusions from measurement data in inquiry-based university physics labs *Int. J. Sci. Educ.* **45** 1
[33] Buffler A, Allie S and Lubben F 2001 The development of first-year physics students' ideas about measurement in terms of point and set paradigms *Int. J. Sci. Educ.* **23** 1137–56
[34] Kaewkhong K, Mazzolini A, Emarat N and Arayathanitkul K 2010 Thai high-school students' misconceptions about and models of light refraction through a planar surface *Phys. Educ.* **45** 97
[35] Frazão C D and Dos Santos Souza W 2024 A proposed experimental activity to determine optical properties of acrylic by using smartphones as measurement instruments *Phys. Teach.* **62** 610
[36] Sullivan M C 2022 Using a smartphone camera to explore ray optics beyond the thin lens equation *Am. J. Phys.* **90** 610
[37] Khoa D X and Bang N H 2019 A low-cost experimental kit for teaching wave optics based on the CDIO approach *Phys. Teach.* **57** 169–72